



Nanometer-Scale Fabrication of Hydrogen Silsesquioxane (HSQ) Films with Post Exposure Baking

Dong-Hyun Kim¹, Se-Koo Kang², Geun-Young Yeom², and Jae-Hyung Jang^{1,*}

¹*School of Information and Communications and WCU Department of Nanobio Materials and Electronics, Gwangju Institute of Science and Technology, 1 Oryongdong, Buk-Gu, Gwangju, 500-712, Korea*

²*SKKU Advanced Institute of Nano Technology, Sungkyunkwan University, Suwon, Gyeonggi-Do, 440-746, Korea*

A nanometer-scale grating structure with a 60-nm-wide gap and 200-nm-wide ridge has been successfully demonstrated on a silicon-on-insulator substrate by using a 220-nm-thick hydrogen silsesquioxane (HSQ) negative tone electron beam resist. A post exposure baking (PEB) process and hot development process with low concentration (3.5 wt%) of tetramethylammonium hydroxide (TMAH) solution were introduced to realize the grating pattern. To study the effects of post exposure baking on the HSQ resist, Fourier transform infrared spectroscopy (FT-IR) and X-ray photoelectron spectroscopy (XPS) analyses were carried out. From the FT-IR and XPS analyses, it was verified that a thin SiO₂ with high cross-linked network structure was formed on the HSQ surface during the PEB step. This SiO₂ layer prevents the formation of unwanted bonds on the HSQ surface, which results in clearly defined grating structures with a 60-nm-gap and 200-nm-wide-ridge on the 220-nm-thick HSQ resist. The nanometer-scale grating pattern was successfully transferred to the 280-nm-thick silicon layer of a silicon-on-insulator (SOI) substrate by using inductively-coupled-plasma-reactive-ion-etching (ICP-RIE).

Keywords: Hydrogen Silsesquioxane, E-Beam Lithography, FT-IR, XPS, Post Exposure Baking Silicon-on-Insulator (SOI).

1. INTRODUCTION

Hydrogen silsesquioxane (HSQ) is widely used as a high resolution negative tone electron-beam resist in the fabrication of electronic devices with gate length shorter than 10 nm as well as in the production of low loss photonic devices.^{1–4} The advantages of HSQ resist include high resistance to dry etching,^{5–6} small granular size,^{7–9} and a relatively convenient pattern transfer process from the resist onto the semiconductor materials. Recently, active research on nanometer-scale processing have been carried out by using electron beam (e-beam) lithography and a HSQ resist to push the limit of the fabrication technology down to a few nano-meters.

Process conditions such as electron beam dose, the thickness of HSQ,^{10–11} baking and developing temperature,¹² concentration of tetramethyl-ammonium hydroxide (TMAH) based developer solution,¹³ types of the developers,¹⁴ and developing time in TMAH solution¹⁵

were varied and the results were analyzed with the aim of achieving optimal resolution of HSQ by using electron beam lithography.

However, most recent studies have been carried out only with HSQ resist thinner than 30 nm. This is typically unsuitable to fabricate silicon photonic devices on silicon-on-insulator (SOI) substrates, as HSQ resist thicker than 200 nm is required to transfer the waveguide pattern on to the silicon layer.^{3–4} Considering that the resolution of the resist is also limited by the resist thickness,¹³ process development to realize nanoscale patterns on a thick (> 200 nm) HSQ resist is also required for the fabrication of nanometer-scale silicon photonic devices.

In this study, a 50-nm-line/space grating pattern with 220-nm-thick HSQ resist was successfully fabricated by introducing a post exposure baking (PEB) process and a hot development process with a TMAH solution (3.5 wt%). A 60-nm-gap with a 200-nm-wide-ridge with a 220-nm-thick HSQ resist were developed and transferred on to a 280-nm-thick Si top layer by using ICP-RIE as shown in the Figure 1. The PEB process, which is commonly

* Author to whom correspondence should be addressed.

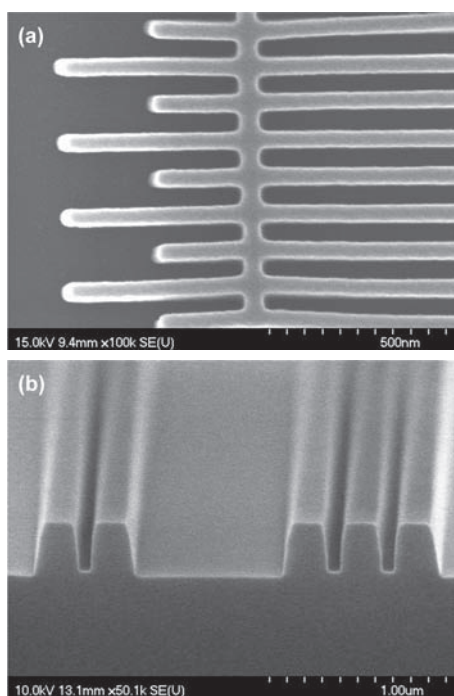


Fig. 1. (a) SEM top view image of grating pattern with 50-nm-wide lines and spaces realized on 220-nm-thick HSQ resist. The sample was developed for 1 min at 50 °C after PEB at 195 °C for 2 min (b) Cross-sectional SEM view of grating pattern with 200-nm-wide line and 60-nm-gap spacing on the SOI substrate. PEB was carried out at 195 °C for 2 min and development was performed for 1 min at 50 °C. For the pattern transfer on to the SOI substrate, ICP-RIE with a SiCl_4/Ar gas mixture was utilized.

employed for producing a negative tone chemically amplified resist (CAR)^{16–17} to increase the contrast of the resist, is introduced to clearly define nanometer-scale grating patterns in the HSQ resist. The nanometer-scale grating patterns were inspected by scanning electron microscopy (SEM) and the effects of PEB on the HSQ resist were investigated by using Fourier transform infrared spectroscopy (FT-IR) and X-ray photoelectron spectroscopy (XPS) analyses.

2. EXPERIMENTAL DETAILS

The HSQ (FOx-12, Dow Corning) resist spun at a speed of 4000 rpm for 60 sec on the SOI substrate resulted in a thickness of 220 nm. The samples covered with HSQ were then prebaked at 150 °C for 2 min on a hot plate. E-beam exposure was carried out using a JEOL JBX-6000FS/E e-beam lithography system with 50 keV acceleration voltage and 1 nA beam current. The grating pattern was designed to comprise periodic 200-nm-wide ridges with 60-nm-wide gaps. The samples after e-beam exposure were baked at 105 °C for 2 min as a PEB step. The samples without PEB (WOPEB) and with PEB were developed with TMAH solution (3.5 wt %) for 1 min at temperatures of 23 °C and 50 °C.

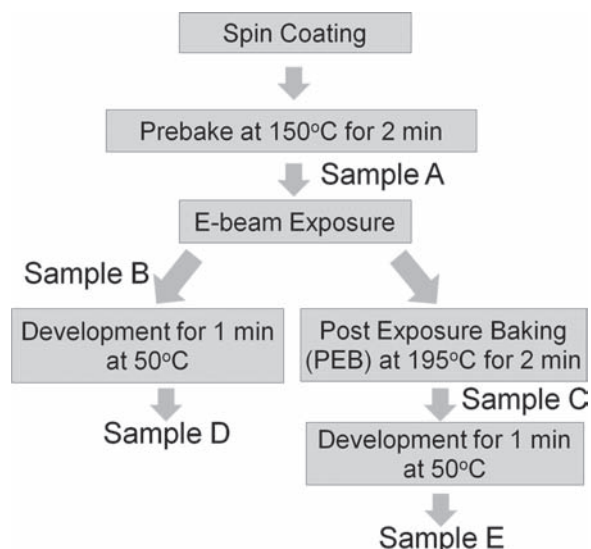


Fig. 2. For the XPS analysis, samples A to E were prepared to investigate the effects of the processing steps.

A parametric study on the PEB temperature was also carried out. To study the effect of the PEB temperature, samples were baked on a hotplate at temperatures of 105 °C, 150 °C, and 195 °C for 2 min after e-beam exposure and were developed at 50 °C for 1 min. The samples were inspected by SEM (Hitachi S-4700) to identify their effects on the HSQ resist.

Additionally, FT-IR spectra were recorded to monitor the chemical change of the resist that occurred during the PEB process step. The FT-IR spectra were obtained by the transmission technique using a ‘Nicolet 5700—ThermoFisher’ spectrometer with a resolution of 2 cm^{-1} . For the FT-IR measurement, prebaked HSQ coated silicon samples were blanket exposed over a 5 mm^2 area with an electron beam lithography system with the same dose ($D = 1500 \mu\text{C}/\text{cm}^2$) as used to fabricate the gratings.

X-ray photoelectron spectroscopy (XPS) was also carried out to inspect the effects of PEB on the HSQ surface in the five cases, as shown in Figure 2. The XPS study was performed using a MultiLab 2000 X-ray photoelectron spectrometer (Thermo Electron) with a Mg K X-ray source ($h = 1253.60 \text{ eV}$). The XPS samples were prepared by e-beam exposure over a 1 mm^2 square area.

The grating pattern on HSQ was transferred to the SOI substrate using an inductively-coupled-plasma-reactive-ion-etching (ICP-RIE) system (Plasmalab system 100, Oxford Instrument Co., UK) with process parameters of $\text{SiCl}_4/\text{Ar} = 10/2.5 \text{ SCCM}$, chamber pressure of 10 mTorr, dc bias of 230 V, and RF power of 50 W.

3. RESULTS AND DISCUSSION

In order to assess the effects of the PEB on the HSQ resist, SEM micrographs of the processed samples were compared. Top view images of the samples with PEB and

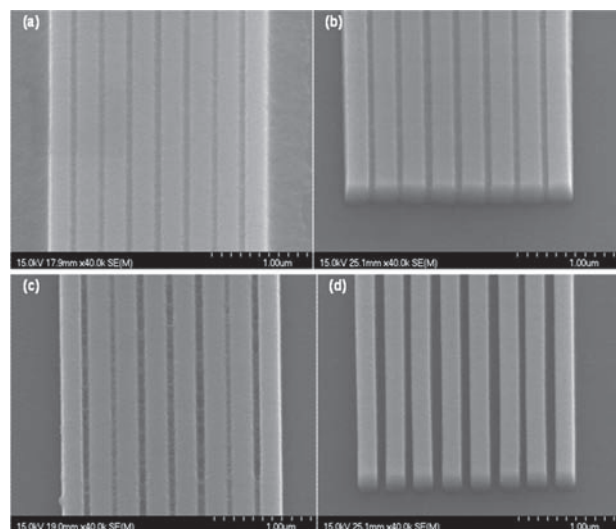


Fig. 3. Comparison of SEM top view images of the developed HSQ resist with the design of 200-nm-width and 80-nm-gap spacing (a) WOPEB sample developed at 23 °C, (b) PEB sample developed at 23 °C, (c) WOPEB sample developed at 50 °C, and (d) PEB sample developed at 50 °C.

without PEB are shown in Figure 3. The effect of PEB can be clearly seen at the edges of the grating patterns developed at room temperature. The WOPEB sample, which was developed at room temperature directly after e-beam exposure without PEB, has residue on the developed area as shown in Figure 3(a). On the contrary, the PEB sample exhibits a clean developed area without any noticeable residue although it was developed at room temperature. The difference can be ascribed to the SiO₂ layer formed on the e-beam exposed surface during the PEB step. The Si-H bonds broken by e-beam irradiation easily make bonds with oxygen in the air, which leads to the formation of SiO₂ layer on the surface. The stable SiO₂ layer prevents further formation of unwanted bonds on the HSQ surface, which are insoluble in TMAH solution.

In Figure 3(c), WOPEB sample developed at an elevated temperature exhibited clean line edges along the pattern. However the residue of HSQ was observed in the 80-nm-gap region. The hot development process improves the contrast along the line edge, but it could not remove the residue at the nanometer-scale gap. However, when the samples were developed at an elevated temperature of 50 °C, the PEB samples exhibited a clearly opened

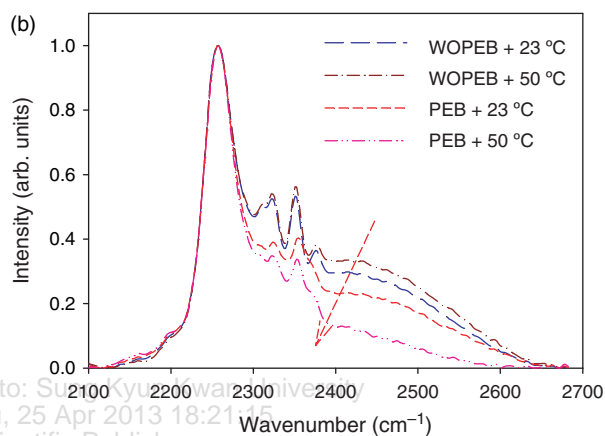
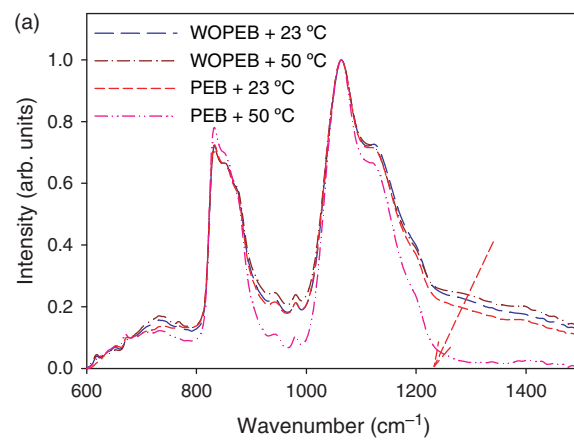


Fig. 5. FT-IR spectra obtained from the HSQ resist process in different conditions. Si-O bending network peak (830 cm⁻¹), Si-O bending cage-like peak (860 cm⁻¹), Si-O stretch network peak (1070 cm⁻¹), and Si-O stretch cage-like peak (1130 cm⁻¹) are shown in (a) and Si-H stretch mode (2250 cm⁻¹) is shown in (b).

nanometer-scale gap as shown in Figure 3(d). Contrary to the WOPEB sample, the PEB process combined with hot development resulted in the best grating patterns with nanometer-scale gap.

It was also shown that the PEB temperature affected the resulting grating structures. Grating patterns fabricated using different PEB temperatures are compared in Figure 4. The grating structures with 200-nm-wide lines and 60-nm-wide gaps exhibited the clearer patterns with the increase of PEB temperature from 105 °C to 195 °C. The SiO₂ layer formed on the HSQ surface during the PEB

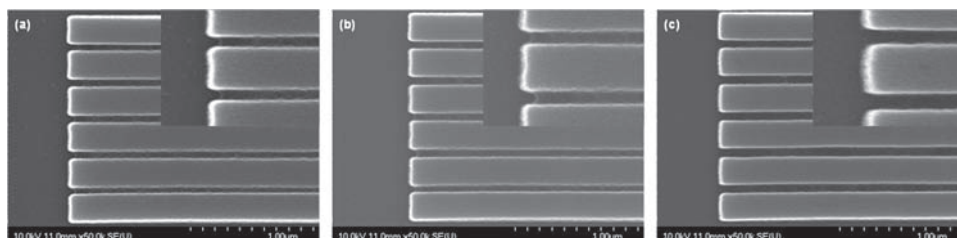


Fig. 4. SEM top view images of the developed PEB samples baked at (a) 105 °C, (b) 150 °C, and (c) 195 °C for 2 min.

process prohibits large molecules to diffuse into the HSQ film and only allows hydrogen to diffuse into the HSQ resist.¹³ The accelerated formation of SiO₂ layer at the higher PEB temperature reduces the likelihood of the generation of unwanted bonds at the HSQ surface. The diffused hydrogen atoms make bonds with the free Si bonds generated by e-beam exposure and form Si-H bonds, which leads to the lower sensitivity and higher contrast.

The chemical change due to each processing step was analyzed on the basis of FT-IR measurement data.

The location of the absorption peaks in the FT-IR spectra is determined by the molecular structures.¹⁸ The FT-IR spectra in Figure 5 exhibit the following absorption peaks:

- (1) Si-H stretch mode (2250 cm⁻¹),
- (2) Si-O stretch cage-like peak (1130 cm⁻¹),
- (3) Si-O stretch network peak (1070 cm⁻¹),
- (4) Si-O bending cage-like peak (860 cm⁻¹), and
- (5) Si-O bending network peak (830 cm⁻¹).

In the normalized FT-IR spectra¹⁹ in Figures 5(a) and (b), WOPEB samples developed at 23 °C and 50 °C

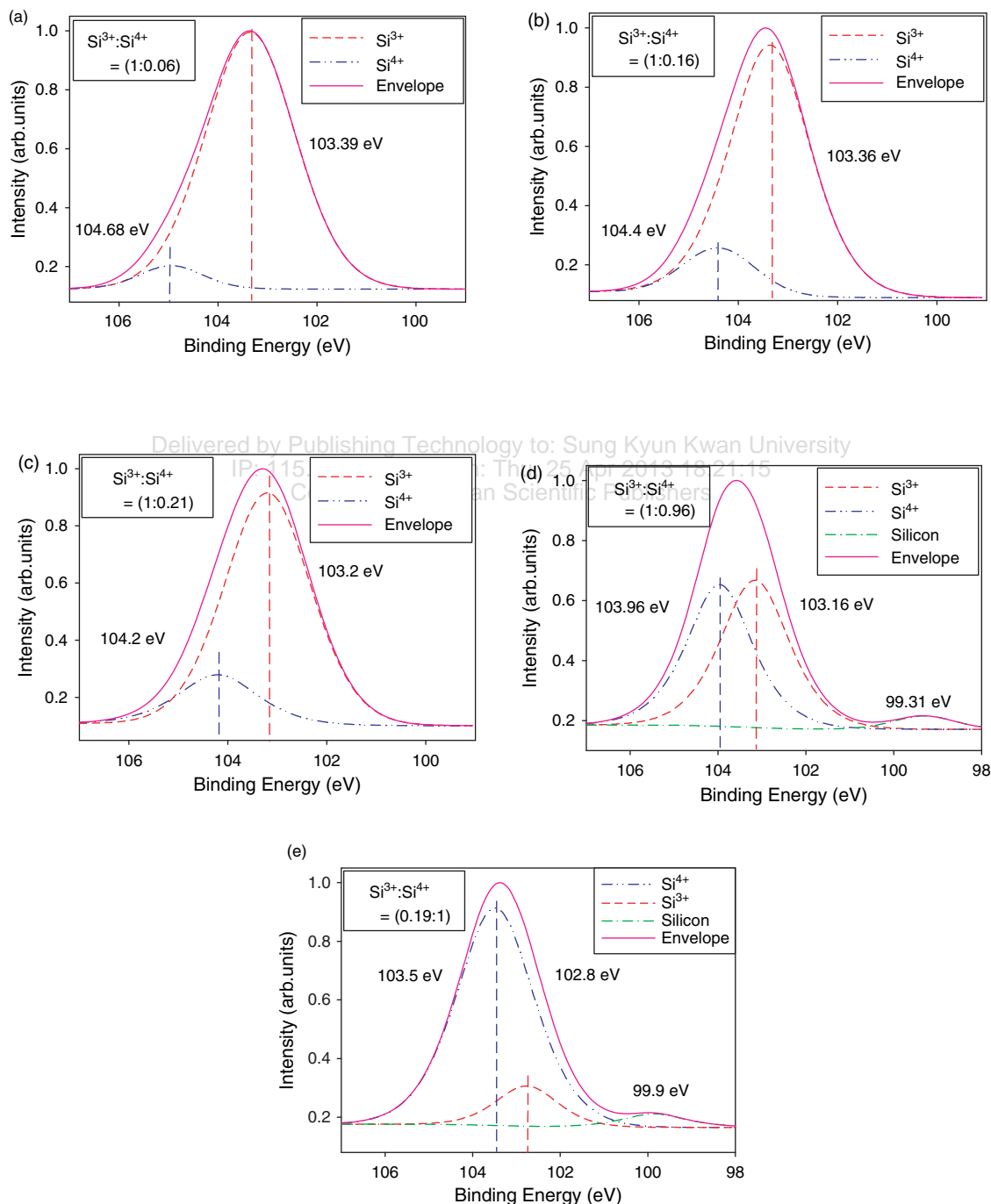


Fig. 6. XPS spectra obtained from samples A to E. (a) sample A (b) sample B (c) sample C (d) sample D (e) sample E.

exhibit higher intensity signal at the skirt of the spectra than the PEB sample developed at 50 °C. This surplus intensity at the skirt can be ascribed to unwanted bonds formed after e-beam exposure due to the instability of the HSQ resist.^{13,19} As a result, the PEB samples have the lower density of unwanted bonds than WOPEB samples.

To shed light on the formation of the SiO₂ layer on the HSQ surface during the PEB process, XPS measurement was carried out. In Figure 6, the XPS spectra show two main peaks corresponding to the high binding energy (103.5 eV~104.95 eV: Si⁴⁺) and the low binding energy (102.8 eV~103.3 eV: Si³⁺).²⁰⁻²¹ The two peaks (Si⁴⁺ and Si³⁺) originate from the strong siloxane bonds (Si–O–Si) and weak silicon hydride bonds (Si–H), respectively.¹⁵

It is known that the silicon hydride bonds can be broken by e-beam exposure and the broken silicon hydride bonds initiate cross-linking reactions.^{7,15} The chemical change due to each processing step can be identified from the relative intensities of the two peaks. Figures 6(a) to (e) show XPS data obtained from samples A to E, respectively. The sample after e-beam exposure (sample B) shows increased Si⁴⁺ peak intensity and decreased Si³⁺ peak intensity compared with the sample before e-beam exposure (sample A). It implied that the strong siloxane bonds (Si–O–Si) with network structure (Si⁴⁺ peak) were formed by e-beam exposure although silicon hydride bonds (Si–H and Si–O⁻) with cage structure (Si³⁺ peak) are still dominant. In other words, the increase of Si⁴⁺ peak intensity in sample C showed that more cross-linked network structures were formed on the surface during the PEB process.²¹

The samples developed in the TMAH based solution (sample D) exhibited the higher Si⁴⁺ peak intensity and the lower Si³⁺ peak intensity compared with the samples before development (sample B). Because silicon hydride bonds (Si–H) and silanol groups (Si–O⁻) dissolve in TMAH solution and form siloxane bonds (Si–O–Si),¹³ the Si⁴⁺ peak intensity is increased and the Si³⁺ peak intensity is decreased after the TMAH development process. As shown in Figure 6(e), Si⁴⁺ peak intensity is much higher than Si³⁺ peak in the PEB sample (sample E), which confirms that cross-linked network structure is dominant at the surface of the PEB sample.

4. CONCLUSION

Grating structures with 200-nm-width and 60-nm-gap spacing were demonstrated on a 220-nm-thick HSQ resist by introducing a PEB process to the normal e-beam lithography process. The improvement in the nanofabrication

process can be ascribed to the effects of the SiO₂ layer formed during the PEB process. By employing XPS and FT-IR, it was confirmed that SiO₂ layer was formed at the surface of HSQ resist during PEB process and the number of unwanted bonds were reduced due to the effect of the SiO₂ layer which stabilizes HSQ surface. By introducing the PEB process together with high temperature development, the potential of the HSQ negative e-beam resist can be fully exploited for the fabrication of high resolution nanometer-scale devices.

Acknowledgment: This work was supported by the World Class University WCU program at GIST through a grant provided by the Ministry of Education, Science and Technology (MEST) of KOREA (No. R31-10026) and a NRF grant (No. 20110017603).

References and Notes

1. I.-B. Baek and J.-H. Yang, *J. Vac. Sci. Technol. B* 23, 3120 (2005).
2. M. Gnan, S. Thoms, D. S. Macintyre, R. M. De La Rue, and M. Sorel, *Electron. Lett.* 44, 115 (2008).
3. S. Xiao, M. H. Khan, H. Shen, and M. Qi, *Opt. Express* 15, 14467 (2007).
4. S. Xiao, M. H. Khan, H. Shen, and M. Qi, *Journal of Lightwave Technology* 26, 228 (2008).
5. L. O'Faolain, M. V. Kotlyar, N. Tripathi, R. Wilson, and T. F. Krauss, *J. Vac. Sci. Technol. B* 24, 336 (2006).
6. D. Park, T. H. Stievater, W. S. Rabinovich, and N. Green, *J. Vac. Sci. Technol. B* 24, 336 (2006).
7. H. Namatsu, M. Nagase, T. Yamaguchi, K. Yamazaki, and K. Kurihara, *J. Vac. Sci. Technol. B* 16, 3315 (1998).
8. T. Barwicz and H. I. Smith, *J. Vac. Sci. Technol. B* 21, 3315 (2003).
9. H. Namatsu, Y. Takahashi, K. Yamazaki, Y. Yamaguchi, M. Nagase, and K. Kurihara, *J. Vac. Sci. Technol. B* 16, 69 (1998).
10. M. J. Word and I. Adesida, *J. Vac. Sci. Technol. B* 21, L12 (2003).
11. V. Sidorkin, A. Grigorescu, H. Salemink, and E. van der Drift, *Microelectron. Eng.* 86, 749 (2009).
12. S. Choi, N. Jin, V. Kumar, and I. Adesida, *J. Vac. Sci. Technol. B* 25, 2085 (2007).
13. W. Henschel, Y. M. Georgiev, and H. Kurz, *J. Vac. Sci. Technol. B* 21, 2018 (2003).
14. D. Lauvernier, J.-P. Vilcot, M. Francois, and D. Decoster, *Microelectron. Eng.* 75, 177 (2004).
15. H.-S. Lee, J.-S. Wi, S.-W. Nam, H.-M. Kim, and K.-B. Kim, *J. Vac. Sci. Technol. B* 27, 188 (2009).
16. P. Sanchis, J. Blasco, A. Martinez, and J. Marti, *Journal of Lightwave Technology* 25, 1298 (2007).
17. Z. Cui, A. Gerardino, M. Gentili, E. DiFabrizio, and P. D. Prewett, *J. Vac. Sci. Technol. B* 16, 3284 (1998).
18. M. Haffner, A. Haug, A. Heeren, M. Fleischer, H. Peisert, T. Chasse, and D. P. Kern, *J. Vac. Sci. Technol. B* 16, 2045 (2007).
19. F. C. M. J. M. Van Delft, *J. Vac. Sci. Technol. B* 20, 2932 (2002).
20. F. G. Bell and L. Ley, *Phys. Rev. B* 37, 8383 (1988).
21. S. Iwata and A. Ishizaka, *J. Appl. Phys.* 79, 6653 (1996).

Received: 30 November 2011. Accepted: 28 March 2012.